SCIENCE AND TECHNOLOGY ORGANIZATION
CENTRE FOR MARITIME RESEARCH AND EXPERIMENTATION

Reprint Series **CMRE-PR-2019-109**

Converted measurements random matrix approach to extended target tracking using X-band marine radar data

Gemine Vivone, Paolo Braca, Karl Granström, Antonio Natale, Jocelyn Chanussot

June 2019

Originally published in:

18th International Conference on Information Fusion, 6-9 July 2015, Washington DC, USA, pp. 976-983.

About CMRE

The Centre for Maritime Research and Experimentation (CMRE) is a world-class NATO scientific research and experimentation facility located in La Spezia, Italy.

The CMRE was established by the North Atlantic Council on 1 July 2012 as part of the NATO Science & Technology Organization. The CMRE and its predecessors have served NATO for over 50 years as the SACLANT Anti-Submarine Warfare Centre, SACLANT Undersea Research Centre, NATO Undersea Research Centre (NURC) and now as part of the Science & Technology Organization.

CMRE conducts state-of-the-art scientific research and experimentation ranging from concept development to prototype demonstration in an operational environment and has produced leaders in ocean science, modelling and simulation, acoustics and other disciplines, as well as producing critical results and understanding that have been built into the operational concepts of NATO and the nations.

CMRE conducts hands-on scientific and engineering research for the direct benefit of its NATO Customers. It operates two research vessels that enable science and technology solutions to be explored and exploited at sea. The largest of these vessels, the NRV Alliance, is a global class vessel that is acoustically extremely quiet.

CMRE is a leading example of enabling nations to work more effectively and efficiently together by prioritizing national needs, focusing on research and technology challenges, both in and out of the maritime environment, through the collective Power of its world-class scientists, engineers, and specialized laboratories in collaboration with the many partners in and out of the scientific domain.

NOTE: The CMRE Reprint series reprints papers and articles published by CMRE authors in the open literature as an effort to widely disseminate CMRE products. Users are encouraged to cite the original article where possible.

Converted Measurements Random Matrix Approach to Extended Target Tracking Using X-band Marine Radar Data

Gemine Vivone*, Paolo Braca*, Karl Granström†, Antonio Natale‡, and Jocelyn Chanussot§
*NATO STO Centre for Maritime Research and Experimentation, 19126 La Spezia, Italy
Emails: {gemine.vivone,paolo.braca}@cmre.nato.int
†Department of Electrical and Computer Engineering, University of Connecticut, Storrs, CT 06269 USA
Email: karl.granstrom@uconn.edu
‡IREA-CNR, 80124 Naples, Italy
Email: natale.a@irea.cnr.it
§GIPSA-Lab, Grenoble Institute of Technology, 38000 Grenoble, France
Email: jocelyn.chanussot@gipsa-lab.grenoble-inp.fr

***Abstract*—Conventional tracking algorithms rely upon the hypothesis of one detection per target for each frame. However, very fine spatial resolution radars represent widespread systems that provides data for which this hypothesis could be no longer valid. This problem is often called in the literature extended target tracking.**

In this paper we propose to use the well-established random matrix theory to deal with this issue. A suitable measurement model to address the radar's measurement noise and its conversion into Cartesian coordinates is proposed. The benefits of the proposed converted measurements - extended target tracking with regard to the problem of the targets' size estimation are demonstrated by using both simulated and real data acquired by an X-band marine radar. Average gains of 75% in the estimation of the targets' cross-range size and 31% for the along-range size are observed by comparing the proposed approach with the one that neglects the sensor's noises.

I. Introduction

Conventional tracking algorithms rely on the point target hypothesis, i.e. there is at most one detection provided by a target per frame. In many cases a target can be represented by a cloud of detections thanks to, for instance, a fine spatial resolution of acquisition systems. Thus, the above-mentioned point target hypothesis is no longer valid. This problem is often called extended target tracking (ETT), and some powerful approaches have already been developed in the literature, see *e.g.* [1]–[5].

A well-established and used ETT framework, under the hypothesis of elliptical target shape, is provided by Koch in [6] where an approximate Bayesian solution to the extended target tracking problem is proposed. Random matrices are exploited to model the ellipsoidal object extensions, which are treated as additional state variables to be estimated. The target kinematic states are modeled using a Gaussian distribution, while the ellipsoidal target extension is modeled using an inverse Wishart distribution. Random matrices are also used to model extended targets under kinematic constraints in [7]. In [8], [9], the authors integrate the use of random matrices into the probabilistic multi-hypothesis tracking framework to address the multi-target tracking problem. Multi-target tracking using random matrices is also addressed in [10], [11].

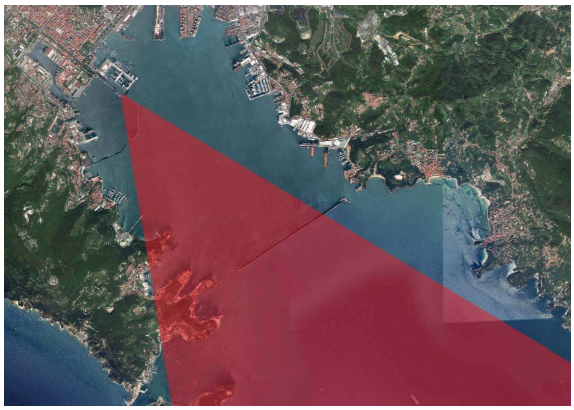

Fig. 1. The X-band marine radar is installed in the Gulf of La Spezia, Italy. The sensor's field of view is shown in red.

In [12] a new random matrix approach is derived to overcome some of the weaknesses in [6], such as sensor inaccuracies that are not taken into account in the original framework. Indeed, if the sensor noise is large in comparison to target size, the lack of modeling may lead to an overestimation of target size as already remarked in [13]. An integration between random matrices and the interacting multiple model estimator is provided in [12]. New measurement and time updates for [12] are proposed in [14] and [15], respectively. An application using real-world radar data, acquired during the recovery operations of the Costa Concordia wreckage in October 2013, and the random matrices framework is reported in [16].

In radar signal processing a very crucial point is the data conversion. The radar measurement of the target are usually

given in polar coordinates, while the target position and dynamics typically are modeled in Cartesian coordinates. The effects of the polar to Cartesian data conversion have to be properly taken into consideration, otherwise the performance of the target tracking may suffer.

In this paper, we investigate how the conversion between polar and Cartesian coordinates can be integrated into the extended target model presented in [12]. A comparison between the proposed approach, the original framework presented in [6], and the one in [12], where the sensor inaccuracies are taken into consideration, is provided. The advantages of the proposed model are demonstrated using simulated data as well as three real world datasets acquired by an X-band marine radar installed in the Gulf of La Spezia, Italy. The radar's field of view is depicted in Fig. I.

The presented estimation results show that, while no considerable gains in the estimation of the targets' kinematic parameters can be found, a great improvement in the targets' size estimation is evident. For targets that sail along a radial path, average gains of 75% in the estimation of the targets' width (cross range size) and 31% for the length (along range size) are observed by comparing the proposed approach with one that does not model the sensor's noise.

The paper is outlined as follows. Sect. II describes the Bayesian extended target modeling, including a coordinate conversion model approach. Sect. III presents the filtering equations that the modeling lead to. The experimental results on both simulated and real data are shown in Sect. IV. Finally, conclusions are drawn in Sect. V.

II. Bayesian Extended Target Modeling

This section is devoted to the description of the proposed measurement model using converted measurements and its integration into the Bayesian extended target tracking framework presented first in [6], and later improved in [12] with the consideration of the sensors' measurement errors. It is worth pointing out that the above-mentioned papers concentrate attention on the track filtering. Estimations under observation-to-track association uncertainty with possible presence of missed detections and false alarms are out-of-scope. The same assumption is made in this paper.

A. State model

The extended target kinematics (position and velocity) are defined in 2D Cartesian coordinates and modeled by the vector $\mathbf{x}_k \triangleq [x_k, \dot{x}_k, y_k, \dot{y}_k]^T$, where x_k, y_k and $\dot{x}_k$, $\dot{y}_k$ are the position and velocity components along the X, Y directions, respectively, and $[\cdot]^T$ is the transpose operator. The extended target's extent (shape and size) is assumed elliptic and is modeled by the positive definite matrix $\mathbf{X}_k$.

Let $\mathbf{Z}^k = \{\mathbf{Z}_m\}_{m=0}^k$ denote all the measurement sets up to and including frame k. The extended target state, i.e. $\mathbf{x}_k$ and $\mathbf{X}_k$, is Gaussian inverse Wishart distributed,

$$p(\mathbf{x}_k, \mathbf{X}_k|\mathbf{Z}^k) = \mathcal{N}(\mathbf{x}_k; \hat{\mathbf{x}}_{k|k}, \mathbf{P}_{k|k})\mathcal{IW}(\mathbf{X}_k; \alpha_{k|k}, \hat{\mathbf{X}}_{k|k}) \quad (1)$$

where $\hat{\mathbf{x}}_{k|k}$ and $\mathbf{P}_{k|k}$ are the expected value and covariance of the Gaussian distribution, and $\hat{\mathbf{X}}_{k|k}$ and $\alpha_{k|k}$ are the expected value and degrees of freedom of the inverse Wishart distribution.

B. Dynamic Model

The target's motion is described by a nearly constant velocity model [17]. The state-update equation is as follows

$$\mathbf{x}_k = \mathbf{F}\ \mathbf{x}_{k-1} + \mathbf{\Gamma}\ \mathbf{w}_k \quad (2)$$

where $\mathbf{F} = \widetilde{\mathbf{F}} \otimes \mathbf{I}_d$, $\mathbf{I}_d$ is the identity matrix with dimension $d \times d$ (i.e. 2×2 in our case), $\otimes$ denotes the Kronecker product,

$$\widetilde{\mathbf{F}} = \begin{bmatrix} 1 & T_s \\ 0 & 1 \end{bmatrix}, \quad (3)$$

T_s is the sampling time, $\mathbf{\Gamma} = \widetilde{\mathbf{\Gamma}} \otimes \mathbf{I}_d$,

$$\widetilde{\mathbf{\Gamma}} = \sigma_{pos} \cdot \begin{bmatrix} T_s^2/2 \\ T_s \end{bmatrix}, \quad (4)$$

and σ_{pos} represents the process noise (equal in both X and Y directions). The process noise $\mathbf{w}_k$ takes into account the target acceleration and the unmodeled dynamics and it is assumed to be Gaussian with zero-mean and identity covariance matrix.

The time evolution of the extent $\mathbf{X}_k$ is modeled as approximately constant over time. This model is accurate for targets that can be assumed to move linearly, i.e. targets that do not turn significantly (a turn causes the extension to rotate). For the scenarios considered in this paper this assumption is true. Motion models for turning targets can be found in related literature, see e.g. [15].

C. Measurement Model Using Converted Measurements

Measurements of the target's positions are usually provided in polar coordinates (i.e. in range and azimuth) for data acquired by radar systems. However, the target motion is typically modeled in Cartesian coordinates. Hence, a conventional linear Kalman filter can be exploited only after the measurements have been converted from polar to Cartesian coordinates. It is important for the tracking results that the effects of this conversion are properly taken into consideration.

The components of the j^{th} measurement vector at frame k are defined as $\boldsymbol{\zeta}_k^j \triangleq \left[r_k^j, \theta_k^j\right]^T$, where r_k^j and θ_k^j are the j^{th} range and azimuth radar measurements at frame k, respectively. These measurements are modeled as the true range and azimuth values, plus measurement errors that are zero-mean Gaussian distributed with standard deviations equal to σ_r and σ_θ, respectively. To convert measurements from polar to Cartesian coordinates we employ the standard coordinate conversion,

$$\mathbf{z}_k^j \triangleq \left[x_k^j,\ y_k^j\right]^T = \left[r_k^j \cos\theta_k^j,\ r_k^j \sin\theta_k^j\right]^T \quad (5)$$

Taking the first order terms of the Taylor series expansion of the standard coordinate conversion, i.e. using linearization, we

obtain the Cartesian coordinate errors, which have zero-mean and covariance matrix [17]

$$\mathbf{R}(\boldsymbol{\zeta}_k^j) = \mathbf{J}(\boldsymbol{\zeta}_k^j)\text{diag}([\sigma_r^2, \sigma_\theta^2])\mathbf{J}^T(\boldsymbol{\zeta}_k^j), \tag{6}$$

where

$$\mathbf{J}(\boldsymbol{\zeta}_k^j) = \begin{bmatrix} \cos\theta_k^j & -r_k^j \sin\theta_k^j \\ \sin\theta_k^j & r_k^j \cos\theta_k^j \end{bmatrix} \tag{7}$$

is the Jacobian matrix, and $\text{diag}(\cdot)$ indicates a diagonal matrix.

For the radar data used in this paper the standard coordinate conversion was empirically found to be sufficient. Other conversions, such as the unbiased one [17], [18], exist and can be exploited if necessary. The proposed approach can be easily generalized to other conversion rules, e.g. the ones shown in [17], [18].

We assume, as done in [6], [12], that at each frame there is a set of n_k independent Cartesian position measurements, denoted $\mathbf{Z}_k = \{\mathbf{z}_k^j\}$. The detection set likelihood is

$$p(\mathbf{Z}_k|n_k, \mathbf{x}_k, \mathbf{X}_k) = \prod_{j=1}^{n_k} p(\mathbf{z}_k^j|\mathbf{x}_k, \mathbf{X}_k). \tag{8}$$

Each detection $\mathbf{z}_k^j$ is modeled as a noisy measurement of a reflection point $\mathbf{y}_k^j$ located somewhere on the extended target. Further, each reflection point is modeled as a point randomly sampled from the target's extension. The detection likelihood is thus

$$p(\mathbf{z}_k^j|\mathbf{x}_k, \mathbf{X}_k) = \int p(\mathbf{z}_k^j|\mathbf{y}_k^j, \mathbf{x}_k, \mathbf{X}_k) p(\mathbf{y}_k^j|\mathbf{x}_k, \mathbf{X}_k) \mathrm{d}\mathbf{y}_k^j \tag{9}$$

In other words, the detection likelihood (9) is the marginalization of the reflection point $\mathbf{y}$ out of the estimation problem.

For the type of radar systems considered here the measurement noise is accurately modeled as zero mean Gaussian,

$$p(\mathbf{z}_k^j|\mathbf{y}_k^j, \mathbf{x}_k, \mathbf{X}_k) = \mathcal{N}(\mathbf{z}_k^j; \mathbf{y}_k^j, \mathbf{R}(\mathbf{y}_k^j)), \tag{10}$$

where $\mathbf{R}(\mathbf{y})$ is the covariance matrix (6) obtained when converting polar radar detections to Cartesian coordinates. Further, the reflection points are accurately modeled as uniform samples from the target shape (valid independently of the targets' extent and of the distance between targets and radar),

$$p(\mathbf{y}_k^j|\mathbf{x}_k, \mathbf{X}_k) = \mathcal{U}(\mathbf{y}_k^j; \mathbf{x}_k, \mathbf{X}_k). \tag{11}$$

As suggested by Feldmann et al [12], for an elliptically shaped target the uniform distribution (11) is approximated by the following Gaussian distribution

$$p(\mathbf{y}_k^j|\mathbf{x}_k, \mathbf{X}_k) = \mathcal{N}(\mathbf{y}_k^j; \mathbf{H}\mathbf{x}_k, \rho\mathbf{X}_k) \tag{12}$$

where ρ is a scaling factor. Here $\mathbf{H}$ is a measurement model that selects the position components in the state vector (i.e. $\mathbf{H} = [\mathbf{I}_d, \mathbf{0}_d]$ where $\mathbf{0}_d$ indicates the null matrix with $d = 2$ in our case). In a simulation study Feldmann et al showed that $\rho = 1/4$ is a good parameter setting. In the results section we will address what is an appropriate parameter setting when using real radar data.

Finally, by combining equations (9), (10) and (12), the likelihood is

$$p(\mathbf{z}_k^j|\mathbf{x}_k, \mathbf{X}_k) = \int \mathcal{N}(\mathbf{z}_k^j; \mathbf{y}_k^j, \mathbf{R}(\mathbf{y}_k^j)) \mathcal{N}(\mathbf{y}_k^j; \mathbf{H}\mathbf{x}_k, \rho\mathbf{X}_k) \mathrm{d}\mathbf{y}_k^j. \tag{13}$$

III. Extended target filtering

In this section we present the time update and measurement update for the models presented in the previous section.

A. Time Update

With the assumed independence between the estimates for centroid kinematics and extension and further assuming independent dynamic models for both of them, the standard Kalman filter prediction equations can be exploited [12], [17]:

$$\hat{\mathbf{x}}_{k|k-1} = \mathbf{F}\hat{\mathbf{x}}_{k-1|k-1}, \tag{14}$$

$$\mathbf{P}_{k|k-1} = \mathbf{F}\mathbf{P}_{k-1|k-1}\mathbf{F}^T + \boldsymbol{\Gamma}. \tag{15}$$

The prediction of the target's extension comes directly from the hypothesis that the extension does not tend to change over time, i.e.

$$\hat{\mathbf{X}}_{k|k-1} = \hat{\mathbf{X}}_{k-1|k-1}. \tag{16}$$

Finally, the prediction of the degrees of freedom parameter $\alpha_{k|k-1}$ is given as [12]

$$\alpha_{k|k-1} = 2 + \exp\left(-T_s/\tau\right)\left(\alpha_{k-1|k-1} - 2\right), \tag{17}$$

where τ is a time constant related to the agility with which the target may change its extension over time.

B. Measurement update

The marginalization (13) is analytically intractable. To achieve a computationally efficient measurement update we make two assumptions. First, assume that in (10) the measurement noise covariance can be approximated as $\mathbf{R}(\mathbf{y}_k^j) \approx \mathbf{R}(\mathbf{H}\mathbf{x}_k)$, i.e.

$$p(\mathbf{z}_k^j|\mathbf{y}_k^j, \mathbf{x}_k, \mathbf{X}_k) \approx \mathcal{N}(\mathbf{z}_k^j; \mathbf{y}_k^j, \mathbf{R}(\mathbf{H}\mathbf{x}_k)). \tag{18}$$

Remark: In general, this approximation is less accurate the larger the distance is between the reflection point $\mathbf{y}$ and the target's position, as given by $\mathbf{H}\mathbf{x}$. This implies that the approximation is less accurate the larger the target is, since a large target means that the distance between the reflection point and position may be large. For the radar sensors and the targets that are considered in this paper, we have empirically found that the approximation is sufficiently accurate. □

Following the assumption, after marginalization (9), we have

$$p(\mathbf{z}_k^j|\mathbf{x}_k, \mathbf{X}_k) = \mathcal{N}(\mathbf{z}_k^j; \mathbf{H}\mathbf{x}_k, \rho\mathbf{X}_k + \mathbf{R}(\mathbf{H}\mathbf{x}_k)). \tag{19}$$

The prior target distribution is Gaussian inverse Wishart,

$$\begin{aligned} p(\mathbf{x}_k, \mathbf{X}_k|\mathbf{Z}^{k-1}) =& \mathcal{N}(\mathbf{x}_k; \hat{\mathbf{x}}_{k|k-1}, \mathbf{P}_{k|k-1}) \\ & \times \mathcal{IW}(\mathbf{X}_k; \alpha_{k|k-1}, \hat{\mathbf{X}}_{k|k-1}). \end{aligned} \tag{20}$$

Second, assume that the following approximation holds,

$$p(\mathbf{z}_k^j|\mathbf{x}_k,\mathbf{X}_k)p(\mathbf{x}_k,\mathbf{X}_k)$$
$$=\mathcal{N}(\mathbf{z}_k^j;\mathbf{H}\mathbf{x}_k,\rho\mathbf{X}_k+\mathbf{R}(\mathbf{H}\mathbf{x}_k))p(\mathbf{x}_k,\mathbf{X}_k|\mathbf{Z}^{k-1}) \quad (21)$$
$$\approx\mathcal{N}(\mathbf{z}_k^j;\mathbf{H}\mathbf{x}_k,\rho\mathbf{X}_k+\mathbf{R}(\mathbf{H}\hat{\mathbf{x}}_{k|k-1}))p(\mathbf{x}_k,\mathbf{X}_k|\mathbf{Z}^{k-1}), \quad (22)$$

i.e. we assume that the measurement noise covariance can be approximated by replacing $\mathbf{x}_k$ with its predicted expected value $\hat{\mathbf{x}}_{k|k-1}$.

Remark: This approximation is trivially satisfied when $\mathbf{R}(\cdot)$ is a constant matrix. In general the assumption holds approximately when $\mathbf{R}(\cdot)$ does not vary too much in the uncertainty region for the extended target. Empirically we have found that, for the sensors and targets considered here, the signal to noise ratio is high enough to make the uncertainty region small enough. □

Under the two assumptions above the measurement update is analogous to the measurement update proposed in [12]. The measurement updated expected value and covariance of the state vector estimate are obtained by a Kalman filter update [12]

$$\hat{\mathbf{x}}_{k|k}=\hat{\mathbf{x}}_{k|k-1}+\mathbf{K}_{k|k-1}(\bar{\mathbf{z}}_k-\mathbf{H}\hat{\mathbf{x}}_{k|k-1}), \quad (23)$$
$$\mathbf{P}_{k|k}=\mathbf{P}_{k|k-1}-\mathbf{K}_{k|k-1}\mathbf{S}_{k|k-1}\mathbf{K}_{k|k-1}^T, \quad (24)$$

where

$$\mathbf{S}_{k|k-1}=\mathbf{H}\mathbf{P}_{k|k-1}\mathbf{H}^T+\frac{\mathbf{Z}_{k|k-1}}{n_k}, \quad (25)$$
$$\mathbf{K}_{k|k-1}=\mathbf{P}_{k|k-1}\mathbf{H}^T\mathbf{S}_{k|k-1}^{-1} \quad (26)$$

are the innovation covariance and the gain, and

$$\mathbf{Z}_{k|k-1}=\rho\hat{\mathbf{X}}_{k|k-1}+\mathbf{R}_k(\mathbf{H}\hat{\mathbf{x}}_{k|k-1}) \quad (27)$$

indicates the predicted covariance of a single measurement. Note that the posterior of the kinematic state conditioned on $\mathbf{x}_k$ is again assumed to be close to a normal distribution.

The updated expected value and degrees of freedom of the extension estimate $\hat{\mathbf{X}}_{k|k}$ are obtained as follows [12]

$$\hat{\mathbf{X}}_{k|k}=\frac{\alpha_{k|k-1}\hat{\mathbf{X}}_{k|k-1}+\widehat{\mathbf{N}}_{k|k-1}+\widehat{\mathbf{Z}}_{k|k-1}}{\alpha_{k|k}}, \quad (28)$$
$$\alpha_{k|k}=\alpha_{k|k-1}+n_k, \quad (29)$$

where

$$\widehat{\mathbf{N}}_{k|k-1}=\hat{\mathbf{X}}_{k|k-1}^{1/2}\mathbf{S}_{k|k-1}^{-1/2}\mathbf{N}_{k|k-1}\left(\mathbf{S}_{k|k-1}^{-1/2}\right)^T\left(\hat{\mathbf{X}}_{k|k-1}^{1/2}\right)^T, \quad (30)$$
$$\widehat{\mathbf{Z}}_{k|k-1}=\hat{\mathbf{X}}_{k|k-1}^{1/2}\mathbf{Z}_{k|k-1}^{-1/2}\overline{\mathbf{Z}}_k\left(\mathbf{Z}_{k|k-1}^{-1/2}\right)^T\left(\hat{\mathbf{X}}_{k|k-1}^{1/2}\right)^T, \quad (31)$$
$$\mathbf{N}_{k|k-1}=\left(\bar{\mathbf{z}}_k-\mathbf{H}\hat{\mathbf{x}}_{k|k-1}\right)\left(\bar{\mathbf{z}}_k-\mathbf{H}\hat{\mathbf{x}}_{k|k-1}\right)^T, \quad (32)$$

and

$$\bar{\mathbf{z}}_k=\frac{1}{n_k}\sum_{j=1}^{n_k}\mathbf{z}_k^j, \quad (33)$$
$$\overline{\mathbf{Z}}_k=\sum_{j=1}^{n_k}\left(\mathbf{z}_k^j-\bar{\mathbf{z}}_k\right)\left(\mathbf{z}_k^j-\bar{\mathbf{z}}_k\right)^T \quad (34)$$

are the centroid measurement and the measurement spread. Note that the marginalized prior density of the target extension is assumed to be an inverse Wishart density [6]. This implies that the posterior is again of the same form.

IV. Results

In this section we present results using both simulated and real experimental data. The experiments are conducted on both simulated and three real datasets acquired by the X-band marine radar installed in the Gulf of La Spezia, Italy. In order to assess the performance of the compared approaches, the automatic identification system (AIS) reports are used as ground truth [19].

The proposed Bayesian ETT method is compared to two other approaches: one random matrix-based tracking algorithm without a model accounting for the sensors' errors, i.e. with $\mathbf{R}=\mathbf{0}$, and another random matrix-based approach that exploits a constant covariance matrix $\mathbf{R}$. The proposed method is here named converted measurements - ETT (CM-ETT). In the case of a constant covariance matrix $\mathbf{R}$ three different possibilities are tested. They are calculated using (6) by setting θ_k^j to the azimuth mean value on the surveillance area, and letting r_k^j assume one of three values. This gives three different matrices: $\mathbf{R}_1$ calculated for targets that move close to the sensor around range 0.5 km; $\mathbf{R}_2$ calculated for range 2 km, corresponding to the middle of the considered surveillance area; and $\mathbf{R}_3$ hypothesizes that the target sails in a longer range area, around 4 km range.

In the experimental results we could not identify any significant differences for the estimates of the state vector $\mathbf{x}_k$, however there are significant differences for the estimates of the extent matrix $\mathbf{X}_k$. Therefore we will only show estimation results for the extent matrix and not for the state vector.

A. X-band Marine Radar Experiment

The X-band marine radar is a coherent linear frequency modulated continuous wave radar [20]. It is a compact and lightweight system, still maintaining a high performance with relatively simple electronics, since the transmitted power is low and constant. The use of pulse compression [21] and a small transmitted power make the radar a compact, quickly deployable, and scalable system, used for research in the areas of target detection and tracking.

The radar has an antenna mounted on a rotor with variable rotating velocity and the possibility to lock and hold the position towards a specific direction with 0.1° accuracy. The main radar parameters are shown in Tab. I.

B. Detection strategy

The data frames acquired by the X-band marine radar were processed by a detector. The detector output is represented by a cloud of detections that represent a target, and these detection clouds are used as input for the three compared tracking algorithms. A conventional maximum likelihood detector is exploited here, and an assumption of conditional independence among the pixels is made. Furthermore, the radar data

TABLE I
MARINE RADAR SPECIFICATIONS

Parameter	Specification
Frequency	9.6 GHz
Bandwidth	Adjustable up to 150 MHz
Range resolution	Δr = 1 m
Antenna type	Rotating slotted waveguide
Azimuth resolution	$\Delta\theta = 1^\circ$
Angular aperture elevation	20°
Gain	32 dBi
Azimuth antenna speed	0 (stopped) up to 40 revolutions per minute
Azimuth angular accuracy	0.1°
Polarization	Linear horizontal
Transmitted power	Adjustable 50 mW - 5 W (17 - 37 dBm)
Pulse repetition frequency	Adjustable 350 Hz - 10 KHz

TABLE II
PARAMETER SETTINGS REAL CASES

Parameter	Value	Specification
T_s	2/5 s	Sampling time
τ	10/5	Agility object size
σ_{pos}	0.2 m s^{-2}	Std. process noise
v_{max}	10 m s^{-1}	Max. velocity
ρ	$1/4$	Scaling factor
σ_r	$\Delta r/2$ (see Tab. I)	Std. noise range
σ_θ	$\Delta\theta/2$ (see Tab. I)	Std. noise azimuth

amplitudes are modeled as exponential distributed with rate parameters $\lambda_t > 0$ under the *target* hypothesis and $\lambda_{nt} > 0$ for the *non-target* case. These parameters characterize the whole exponential distributions and are estimated by the means of the *k-means* clustering algorithm [22].

C. Real X-band Marine Radar Data

Experiments were conducted using three different datasets. Dataset 1 contains detections from *Grand Holiday*, a Portuguese passenger ship of dimensions 222 m × 32 m with maritime mobile service identity (MMSI) equal to 255803790. Dataset 2 contains detections from an Italian vessel called *Palinuro*, with length 59 m, width 10 m, and MMSI = 247939000. Lastly, dataset 3 contains detections from a cargo ship called *Fabio Duo*. Its size is 80 m × 16 m with MMSI = 247241500. The AIS ground truth and the estimated tracks provided by the CM-ETT algorithm for the three considered datasets are depicted in Fig. 2.

Initially, we determine an appropriate value for the parameter ρ (cf. (12)). Two values of ρ are tested using the CM-ETT approach. In a simulation study presented by Feldmann et al [12], it is suggested to use $\rho = 1$ to model a Gaussian spread of the detections, while $\rho = 1/4$ models a uniform distribution. Fig. 3 clearly shows that the CM-ETT with $\rho = 1/4$ performs better obtaining a closer match with the AIS ship information. This experimental analysis confirms that data with a uniform detection spread is best modeled by $\rho = 1/4$. In the remainder of the paper, the compared extended target filters are implemented with $\rho = 1/4$. The other tracking parameters used in the experiments are shown in Tab. II.

Selected results from the *Grand Holiday* dataset are provided in Fig. 4. We only compare results using the proposed

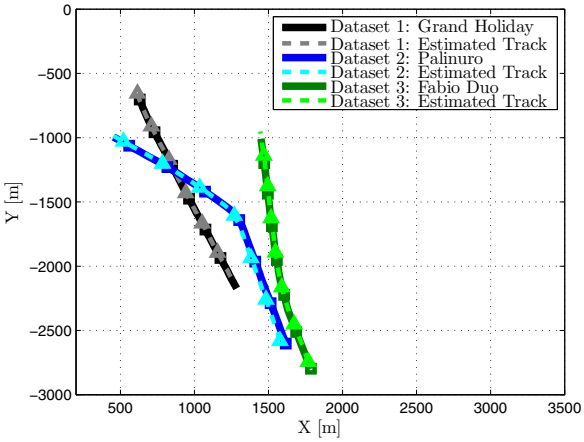

Fig. 2. AIS tracks (solid line with square markers) and target positions estimated by the CM-ETT (dashed line with triangular markers) for the three analyzed datasets.

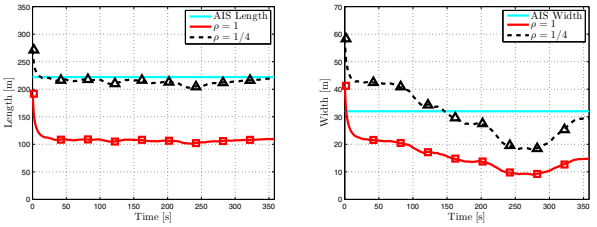

(a) (b)

Fig. 3. (a) Length and (b) width estimation for the CM-ETT using $\rho = 1$ (red solid line) and $\rho = 1/4$ (black dashed line) on the *Grand Holiday* dataset.

approach and using $\mathbf{R} = \mathbf{0}$, because showing all results makes the figures too cluttered. The advantages of properly accounting for the polar measurement noise is evident. In this dataset the target is moving away from the sensor in an almost radial direction, see Fig. 2. Due to the almost radial target trajectory the benefits of CM-ETT over $\mathbf{R} = \mathbf{0}$ are only clear for the estimated width. The benefits are biggest when the sensor to target range is longer.

Length and width estimates for all the filters for the *Grand Holiday* dataset are shown in Fig. 5. There is little difference when it comes to the length estimates, however for the width estimates there are considerable differences. Comparing the proposed approach with the one using $\mathbf{R} = \mathbf{0}$ or the one using $\mathbf{R}_1$ it is clear that the longer the sensor to target range is, the greater the advantages of the proposed model are. Both $\mathbf{R} = \mathbf{0}$ and $\mathbf{R}_1$ result in the width being overestimated. Using $\mathbf{R}_3$ gives the opposite behavior, i.e. the width is underestimated. Finally, $\mathbf{R}_2$ gives a performance that underestimates the width, although the performance is slightly better than $\mathbf{R}_3$.

The results for all the three datasets are summarized as absolute error histograms of the width and length estimates in Fig. 6. Gaussian approximations of these histograms are also

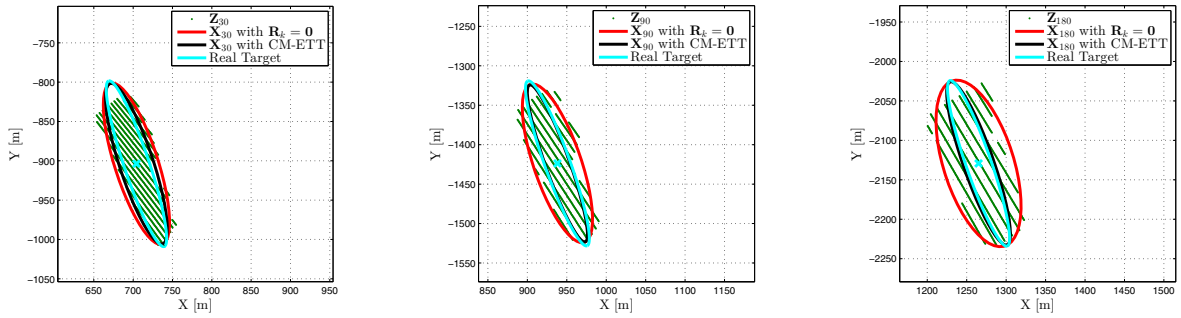

(a) Frame 30 (b) Frame 90 (c) Frame 180

Fig. 4. Estimated ellipsoids provided by the CM-ETT, the $\mathbf{R} = 0$ approach, and the ground truth on the *Grand Holiday* dataset.

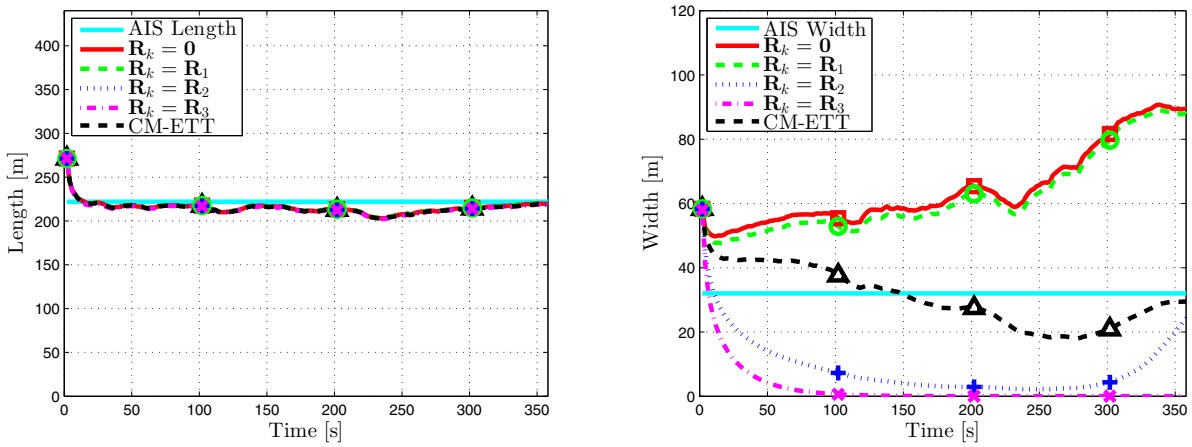

(a) (b)

Fig. 5. (a) Length and (b) width estimations for the compared approaches on the *Grand Holiday* dataset.

shown in the figure. The results for $\mathbf{R}_1$ and $\mathbf{R}_3$ are worse than the results for $\mathbf{R}_2$, therefore we only compare the proposed CM-ETT filter to $\mathbf{R}_2$ and $\mathbf{R} = \mathbf{0}$. The mean width errors are 9.4 m for the CM-ETT algorithm, 21.4 m for the $\mathbf{R}_2$ method, and 37.5 m in the case of the $\mathbf{R} = \mathbf{0}$ approach. The mean length errors are 9.3 m, 10.4 m, and 13.4 m, respectively.

It is evident that by properly modeling the polar measurement noise the errors in both width and length are significantly reduced. For the data used here, the average gains of the proposed CM-ETT approach are 75% compared to the $\mathbf{R} = \mathbf{0}$ approach and 56% with respect to $\mathbf{R}_2$ for the targets' width estimation accuracy, while advantages of 31% and 11%, respectively, can be observed for the targets' length estimation accuracy.

For the considered type of radar the measurement noise is larger in the cross-range direction compared to the along range direction. Due to the shape of the La Spezia Gulf, and the radar position, all of the true tracks mostly follow radial directions. The sensor's uncertainty is largest in the cross-range direction, and it is because of this that we see larger gains for the width estimates than for the length estimates. To test the performance of the proposed model for targets that do not follow radial directions, a radar simulation model was constructed. This is the topic of the next section.

D. Simulated Data

A ship with length 80 m and width 30 m is simulated using a nearly constant velocity model [17] with zero-mean Gaussian noise described by the parameter σ_{pos}, see Eq. (2). The detections were simulated using a Gaussian model with scaling parameter $\rho = 1$ and additive zero-mean Gaussian noise. The noise was simulated in polar coordinates with standard deviations σ_r and σ_θ for the range and azimuth dimensions, respectively. The simulator parameters are shown in Tab. III.

First, the target is simulated as sailing in a radial direction from 1 km to 4 km. Fig. 7 shows the length and width estimation provided by the compared approaches. Because the simulated trajectory is radial with respect to the radar position, and the along-range inaccuracy is less than the cross-range one, no difference is observable for the estimates of the target's length. The advantages are instead clear for the estimates of the target's width, and the longer the sensor to target range

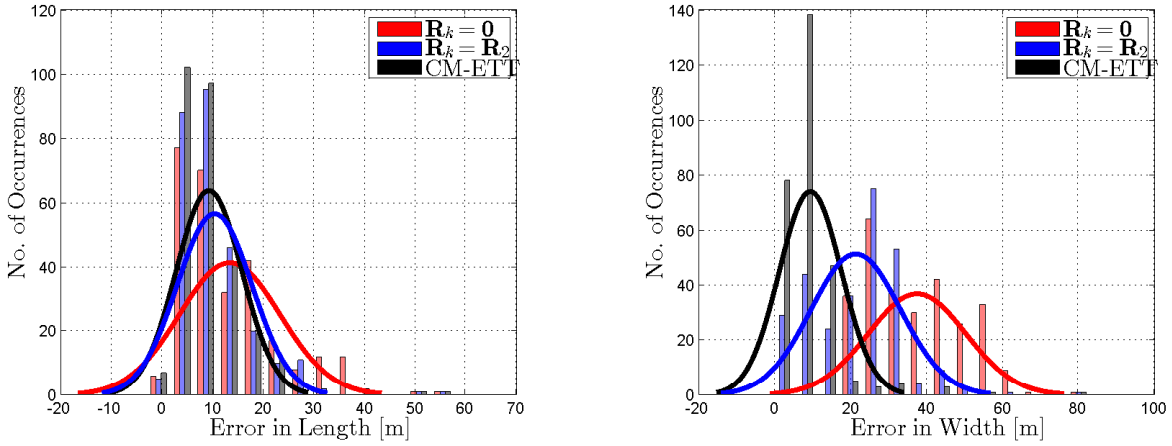

(a) (b)

Fig. 6. Histograms of absolute errors in (a) length and (b) width for the $\mathbf{R} = \mathbf{0}$, the $\mathbf{R} = \mathbf{R}_2$, and the CM-ETT approaches calculated on all the datasets. The solid lines on the foreground indicate the Gaussian fitting of the histograms.

TABLE III
PARAMETER SETTINGS SIMULATOR

Parameter	Value	Specification
T_s	2 s	Sampling time
σ_{pos}	10^{-4} m s^{-2}	Std. process noise
Σ	$\begin{bmatrix} 0.6653 & -0.6453 \\ -0.6453 & 1.1764 \end{bmatrix} \cdot 10^3$	Cov. matrix
k_{max}	400	Num. of frames
N_d	2000	Num. detects. frame
σ_r	0.5 m	Std. noise range
σ_θ	0.5°	Std. noise azimuth

is, the greater the advantages of the proposed model are. With the exception of the results using $\mathbf{R}_2$, these results are similar to the experimental results in Fig. 5, which shows that the simulation model can generate detections that are a realistic model of the real world radar detections.

The second test case simulates the target sailing in an almost constant range track. Because we simulate an almost constant range track the opposite width/length estimation results are expected with respect to the previous test case. Fig. 8 shows the length and width estimation provided by the compared approaches. Again, the CM-ETT shows its ability to properly estimate both the length and width parameters. As expected, considerable advantages are shown for the cross-range size estimation (length), while comparable performance can be pointed out for the estimation of the width parameter (along-range size).

We therefore conclude that the simulation study shows that the proposed CM-ETT gives improved performance both for the cross-range size and the along-range size, regardless of whether the target sails in a radial track or sails with constant range.

V. CONCLUSIONS

In this paper we considered extended target tracking using data from high resolution X-band marine radar. A measurement model that properly takes into account the radar's measurement noises and the data conversion from polar to Cartesian coordinates was proposed. This model is suitable for extended target tracking in the random matrix framework.

The proposed algorithm was compared to previous work using both simulated data and real world experimental data acquired by an X-band marine radar. Estimation performance for the kinematic parameters is comparable to previous work, however the proposed approach shows significant improvements for the estimation of the extent parameters. Compared to previous work the average gains of the proposed approach assessed on real data are up to 75% for the cross-range size and up to 31% for the along-range size.

REFERENCES

[1] K. Gilholm and D. Salmond, "Spatial distribution model for tracking extended objects," *IEE Proc. - Radar, Sonar Navig.*, vol. 152, no. 5, pp. 364–371, Oct. 2005.

[2] Y. Boers, H. Driessen, J. Torstensson, M. Trieb, R. Karlsson, and F. Gustafsson, "Track before detect algorithm for tracking extended targets," *IEE Proc. - Radar, Sonar Navig.*, vol. 153, no. 4, pp. 345–351, Aug. 2006.

[3] R. Mahler, "PHD filters for nonstandard targets, I: Extended targets," in *Proc. of the* 12^{th} *Intern. Conf. on Inform. Fusion (FUSION)*, Seattle, WA, Jul. 2009, pp. 915–921.

[4] K. Granström, C. Lundquist, and O. Orguner, "Extended target tracking using a Gaussian-mixture PHD filter," *IEEE Trans. Aerosp. Electron. Syst.*, vol. 48, no. 4, pp. 3268–3286, Oct. 2012.

[5] M. Baum and U. D. Hanebeck, "Extended object tracking with random hypersurface models," *IEEE Trans. Aerosp. Electron. Syst.*, vol. 50, no. 1, pp. 149–159, Jan. 2014.

[6] J. W. Koch, "Bayesian approach to extended object and cluster tracking using random matrices," *IEEE Trans. Aerosp. Electron. Syst.*, vol. 44, no. 3, pp. 1042–1059, Apr. 2008.

[7] J. W. Koch and M. Feldmann, "Cluster tracking under kinematical constraints using random matrices," *Robot. Auton. Syst.*, vol. 57, no. 3, pp. 296–309, Mar. 2009.

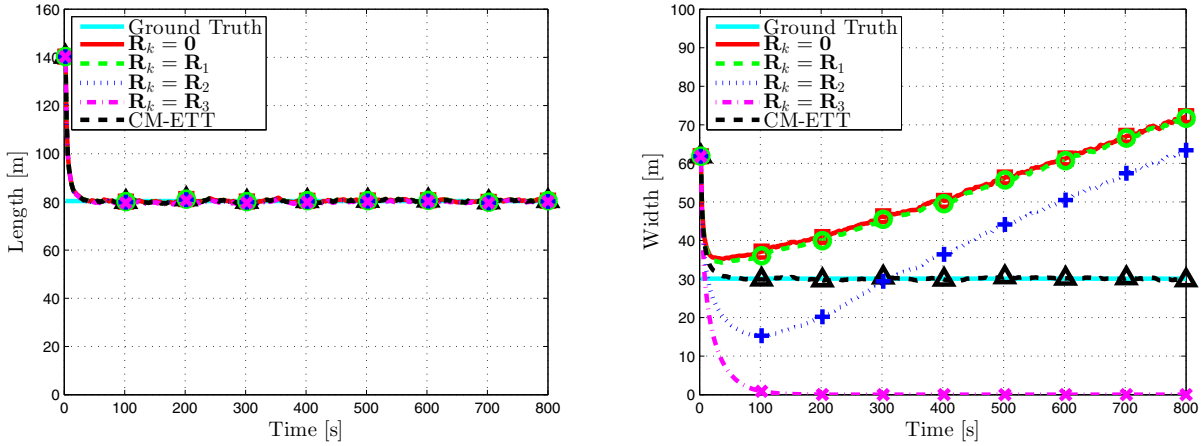

Fig. 7. (a) Length and (b) width estimations for the compared approaches on simulated data for a target that follows a radial track.

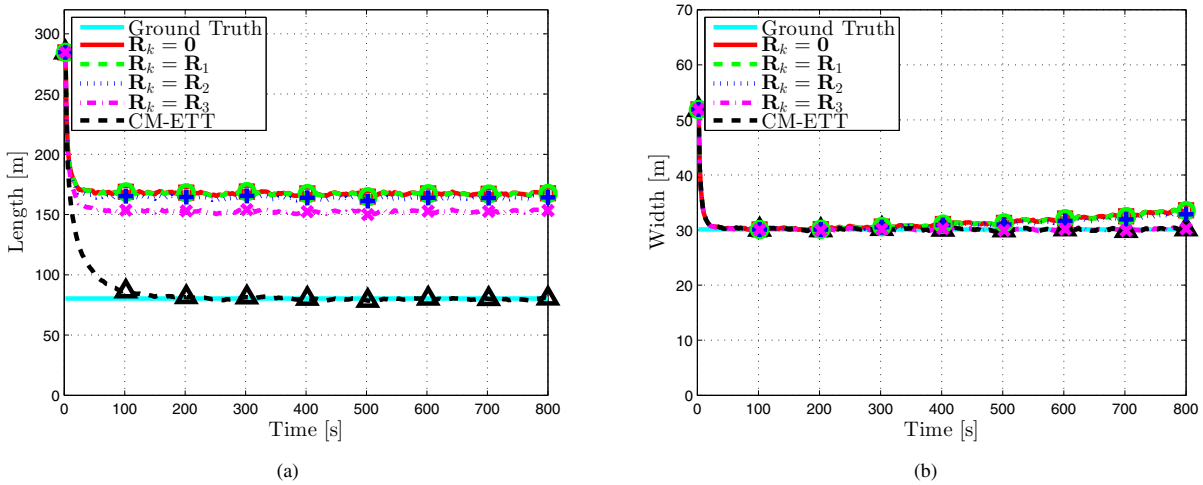

Fig. 8. (a) Length and (b) width estimations for the compared approaches on simulated data for a target that follows an almost along constant range track.

[8] M. Wieneke and J. W. Koch, "Probabilistic tracking of multiple extended targets using random matrices," in *Proc. of SPIE Conf. on Signal Proc. of Small Targ.*, Orlando, FL, Apr. 2010.

[9] ——, "A PMHT approach for extended objects and object groups," *IEEE Trans. Aerosp. Electron. Syst.*, vol. 48, no. 3, pp. 2349–2370, Jul. 2012.

[10] K. Granström and U. Orguner, "A PHD filter for tracking multiple extended targets using random matrices," *IEEE Trans. Signal Process.*, vol. 60, no. 11, pp. 5657–5671, Nov. 2012.

[11] C. Lundquist, K. Granström, and U. Orguner, "An extended target CPHD filter and a gamma Gaussian inverse Wishart implementation," *IEEE Journal of Selected Topics in Signal Processing, Special Issue on Multi-target Tracking*, vol. 7, no. 3, pp. 472–483, Jun. 2013.

[12] M. Feldmann, D. Franken, and J. W. Koch, "Tracking of extended objects and group targets using random matrices," *IEEE Trans. Signal Process.*, vol. 59, no. 4, pp. 1409–1420, Apr. 2011.

[13] B. Errasti-Alcala and P. Braca, "Track before Detect algorithm for tracking extended targets applied to real-world data of X-band marine radar," in *Proc. of the* 17^{th} *Intern. Conf. on Inform. Fusion (FUSION)*, Salamanca, Spain, Jul. 2014.

[14] U. Orguner, "A variational measurement update for extended target tracking with random matrices," *IEEE Trans. Signal Process.*, vol. 60, no. 7, pp. 3827–3834, Jul. 2012.

[15] K. Granström and O. Orguner, "New prediction for extended targets with random matrices," *IEEE Trans. Aerosp. Electron. Syst.*, vol. 50, no. 2, pp. 1577–1589, Apr. 2014.

[16] K. Granström, A. Natale, P. Braca, G. Ludeno, and F. Serafino, "PHD extended target tracking using an incoherent X-band radar: Preliminary real-world experimental results," in *Proc. of the* 17^{th} *Intern. Conf. on Inform. Fusion (FUSION)*, Salamanca, Spain, Jul. 2014.

[17] Y. Bar-Shalom, P. Willett, and X. Tian, *Tracking and Data Fusion: A Handbook of Algorithms*. Storrs, CT: YBS Publishing, Apr. 2011.

[18] S. Bordonaro, P. Willett, and Y. Bar-Shalom, "Decorrelated unbiased converted measurement Kalman filter," *IEEE Trans. Aerosp. Electron. Syst.*, vol. 50, no. 2, pp. 1431–1444, Apr. 2014.

[19] S. Maresca, P. Braca, J. Horstmann, and R. Grasso, "Maritime surveillance using multiple high-frequency surface-wave radars," *IEEE Trans. Geosci. Remote Sens.*, vol. 52, no. 8, pp. 5056–5071, Aug. 2014.

[20] M. I. Skolnik, *Radar handbook*. McGraw-Hill, Incorporated, 1970.

[21] D. Wehner, *High resolution radar*. Artech House, 1987.

[22] A. K. Jain, M. N. Murty, and P. J. Flynn, "Data clustering: a review," *ACM Comput. Surv.*, vol. 31, no. 3, pp. 264–323, Sep. 1999.

Document Data Sheet

Security Classification		Project No.
Document Serial No.	**Date of Issue**	**Total Pages**
CMRE-PR-2019-109	June 2019	8 pp.

Author(s)

Gemine Vivone, Paolo Braca, Karl Granström, Antonio Natale, Jocelyn Chanussot

Title

Converted measurements random matrix approach to extended target tracking using X-band marine radar data

Abstract

Conventional tracking algorithms rely upon the hypothesis of one detection per target for each frame. However, very fine spatial resolution radars represent widespread systems that provide data for which this hypothesis could be no longer valid. This problem is often called in the literature extended target tracking. In this paper we propose to use the well-established random matrix theory to deal with this issue. A suitable measurement model to address the radar's measurement noise and its conversion into Cartesian coordinates is proposed. The benefits of the proposed converted measurements - extended target tracking with regard to the problem of the targets' size estimation are demonstrated by using both simulated and real data acquired by an X-band marine radar. Average gains of 75% in the estimation of the targets' cross-range size and 31% for the along-range size are observed by comparing the proposed approach with the one that neglects the sensor's noises.

Keywords

Target tracking, radar tracking, mathematical model, noise, estimation, covariance matrices

Issuing Organization

NATO Science and Technology Organization
Centre for Maritime Research and Experimentation

Viale San Bartolomeo 400, 19126 La Spezia, Italy

[From N. America:
STO CMRE
Unit 31318, Box 19, APO AE 09613-1318]

Tel: +39 0187 527 361
Fax:+39 0187 527 700

E-mail: library@cmre.nato.int